Eleventh International Conference on Computational Fluid Dynamics (ICCFD11), Maui, Hawaii, USA, July 11-15, 2022
ICCFD11-2022-2001

A Time-accurate, Fast-running CFD Method for the Prediction of A Full Aircraft Flutter Boundary

H. Q. Yang*, Ben Armstrong**
Corresponding author: hq.yang@cfd-research.com
*, ** CFD Research Corporation, Huntsville, AL 35806, USA

The F-16 has a documented history of exhibiting LCOs for certain configurations at specific flight conditions, which has prompted a significant research effort using this configuration. The Open Source Fighter configuration of F-16 was investigated in this study by a time-accurate and fast-running CFD method. The geometry is based on publicly available data for the F-16. Our focus is on the capability of predicting the flutter boundary and then LCO. First, an efficient and robust fluid modal method through the use of a CFD solver is developed to reduce the fully-coupled aeroelasticity problem to a second-order multi-degree-of-freedom (DOF) system while maintaining dominant nonlinearity and effects of all desired DOFs. A technique for rapid extraction of nonlinear fluid modal mass, damping, and stiffness from a CFD solver is shown. These fluid mass, damping, and stiffness are then used to construct a system of ordinary differential equations, thereby replacing the need for coupled CFD/CSD simulations. The developed method is then used to rapidly predict the flutter boundary of a full F-6 aircraft flutter boundary.

Keywords: Numerical Algorithms, Computational Fluid Dynamics, Aeroelasticity

1 Introduction

Accurate analysis of complex flows and the associated aeroelastic response is necessary for the design of next-generation flight vehicles. The coupling of computational fluid dynamics (CFD) solvers and computational structure dynamics (CSD) solvers can give accurate aeroelastic simulations. However, the increase in accuracy comes with a significant additional increase in computational cost. To mitigate this increased cost, the solution runs time, and the total number of solutions generated needs to be minimized. Reduced-order modeling (ROM) is an accurate and cheap alternative to CFD/CSD simulations to study the dynamic aeroelastic response [1][2].

In this paper, an innovative "nonlinear fluid modal method" will be presented to rapidly predict and offer unique physical insight into the nonlinear aeroelasticity of aircraft [3-5]. The distinguishing factors of this effort are: (1) It is physics-based so that changes in aerodynamics, mass, inertia, and center of gravity are accounted for. (2) It is time-accurate and fast running. The coupled CFD/CSD problem is reduced to a set of ordinary differential equations, which can be solved in a matter of seconds compared to several hundred CPU hours. (3) It is CFD/CSD code independent. Any existing CFD solver can be used to build the nonlinear fluid modal model. (4) It is applicable to any geometry and flight condition.

2 Problem Statement

Limit-cycle oscillation (LCO) is a limited-amplitude, self-sustaining oscillation produced by an aero-structural interaction. LCO results in an undesirable airframe vibration and limits the performance of the flight vehicle. Our fluid modal method reduces the fully coupled aeroelasticity problem to an Ordinary Differential Equation (ODE) that is solved fast and efficiently. In this study, the Open Source Fighter configuration of F-16 was investigated. The geometry is based on publicly available data for the F-16. The

F-16 has a documented history of exhibiting LCOs for certain configurations at specific flight conditions, which has prompted a significant research effort using this configuration. Our focus will be on the capability of predicting the flutter boundary and then LCO.

2.1 Simulation Model

The CFD mesh consists of 4.5 million cells of mixed elements and can be seen in Figure 1. An adiabatic no-slip wall boundary condition is applied on the Wing, Fuselage, and Tip Launcher Rail. A far-field boundary condition is applied to the outer boundary of the fluid domain. The freestream initial conditions are listed as follows: Mach = 0.96, Q (dynamic pressure) = 27 kPa, Density = 0.6 kg/m^3, Velocity = 300 m/s, and Altitude = 6864 m.

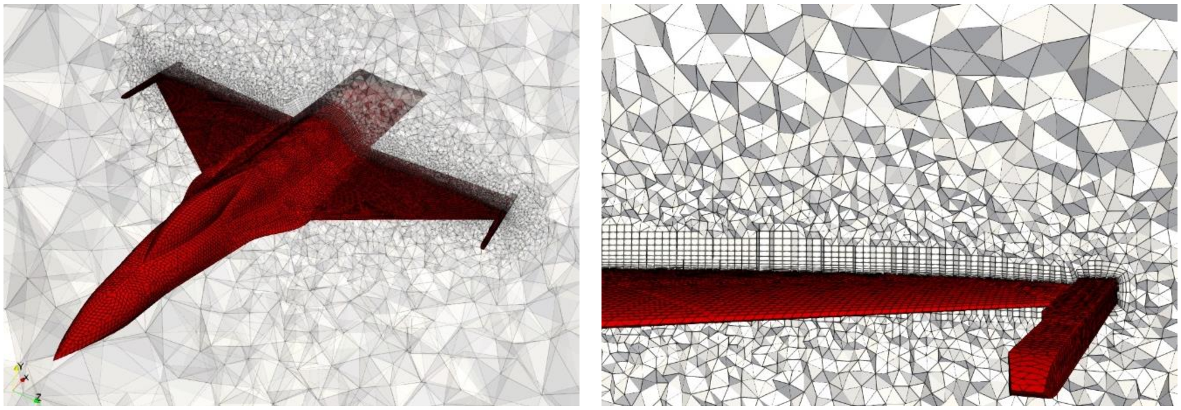

Figure 1. CFD mesh of the Open Source Fighter

The structural model shown in Figure 2 contains 10 modal shapes and has three structural components: Fuselage, Wing, and Stores. Stores are a pair of under-wing fuel tanks whose aerodynamic effects are neglected in the current CFD model.

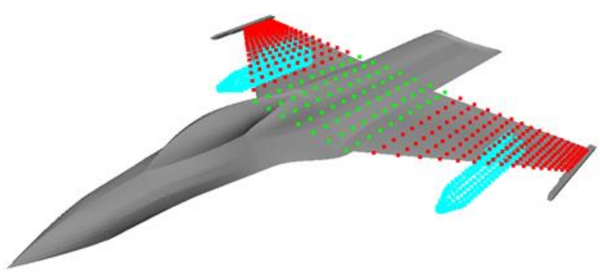

Figure 2. Structural Model of the Open Source Fighter: Fuselage (green), Wing (red), and Stores (light blue)

The structural model shown in Figure 3 shows the first 4 modal shapes.

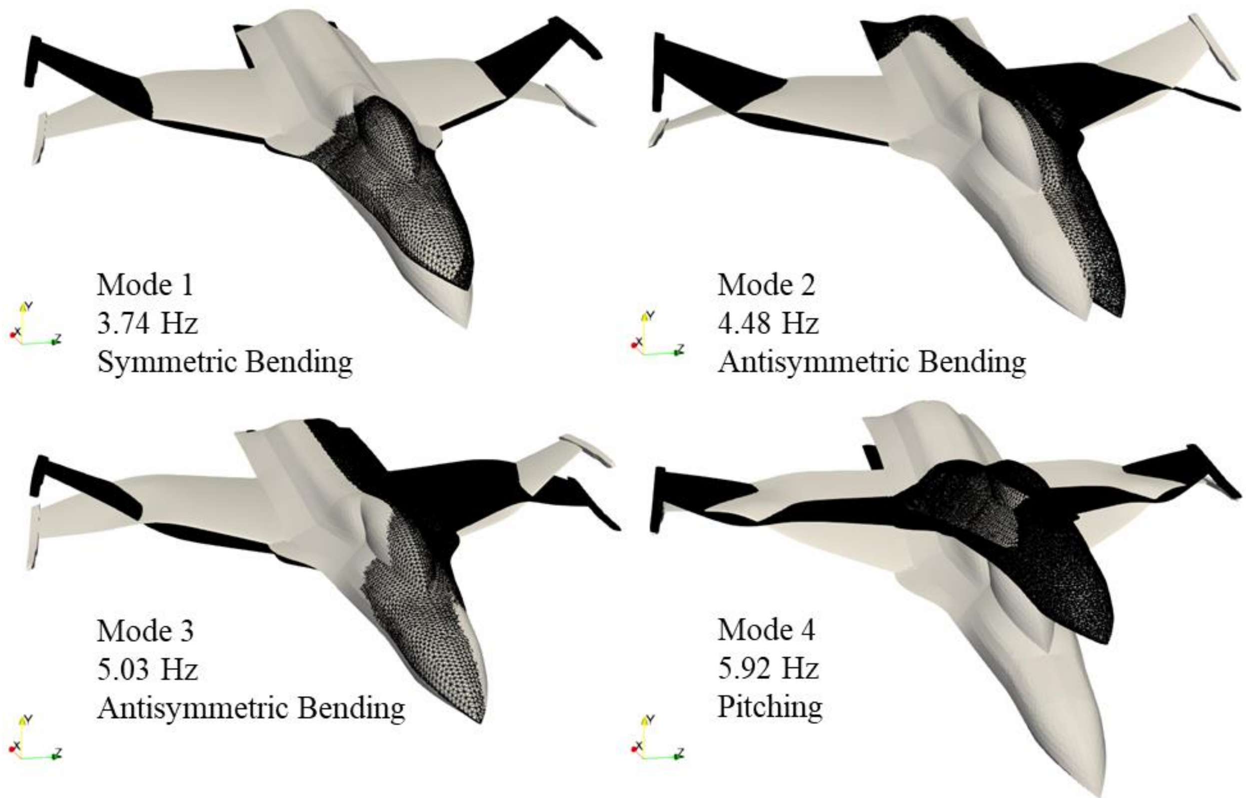

Figure 4. Structural Mode Shapes of the First Four Modes of the Open Source Fighter

Procedure for the Flutter Prediction Using Our Fluid Modal Method [3-5]
The process employed for the demonstration of the nonlinear fluid modal method developed in this study can be broken down into the following five main steps:

1. Extract the fluid stiffness matrix, k;
2. Identify possible couplings between modes;
3. Calculate the critical dynamic pressure Q values and frequencies with the nonlinear fluid modal method
4. Run the fully-coupled FSI simulation;
5. Analyze and compare the predictions from the fully-coupled solution and the fluid modal method solution.

2.2 <u>Efficient Flutter Prediction Using Fluid Modal Method</u>

Formulation of Decoupled Equation

Our approach can be best explained with one degree-of-freedom system, as shown in Figure 4, where a 2D airfoil with plunging degree-of-freedom (y) is subject to fluid flow.

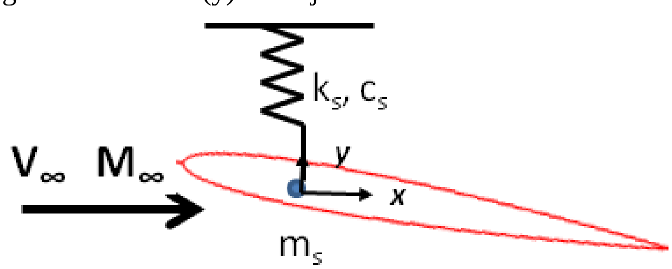

Figure 4. A demonstration example of an airfoil with a vertical degree of freedom in a flow field.

The dynamics equation for the airfoil's plunging motion can be written as:

$$m_s\ddot{y} + c_s\dot{y} + k_s y = F_y(y, \dot{y}, \ddot{y}) \tag{1}$$

where m_s, c_s, and k_s are the mass, damping coefficient, and stiffness of the airfoil structure, respectively. The right-hand side F_y is the integrated aerodynamic force in the y-direction and is a function of the airfoil motion. In our approach, we express

$$F_y(y, \dot{y}, \ddot{y}) = F_y^{\ rig} + [F_y(y, \dot{y}, \ddot{y}) - F_y^{\ rig}] \tag{2}$$

with F_y^{rig} as the aerodynamic force acting on the rigid airfoil without any motion. Presently, the existence of the second term in Equation (2) is purely due to the motion of the airfoil. We then express it as:

$$F_y(y, \dot{y}, \ddot{y}) - F_y^{\ rig} = -m_f\ddot{y} - c_f\dot{y} - k_f y \tag{3}$$

The subscript f represents a fluid quantity. Now, combining equations (1-3) gives us:

$$(m_s + m_f)\ddot{y} + (c_s + c_f)\dot{y} + (k_s + k_f)y = F_y^{\ rig} \tag{4}$$

It is observed that the fully-coupled system has been profoundly simplified into a simple structural dynamics problem with modified mass, damping, and stiffness. Most importantly, the forcing is the aerodynamic force under rigid body conditions, which can be obtained on a routine basis using any CFD tool. For a small displacement y, the fluid mass, damping, and stiffness are constant, and the flutter instability can be determined from the condition of zero total damping. When the structural deformation is large, we can extract the fluid properties as:

$$m_f = m_f(\ddot{x});\ \ c_f = c_f(\dot{x});\ k_f = k_f(x) \tag{5}$$

Now, Equation (4) is a time-accurate, fast-running algorithm for describing the aeroelastic response of the aircraft structures and for defining critical flight conditions.

Extraction of Fluid Mass, Damping, and Stiffness

The fluid side of the decoupled system can be written as follows.

$$-F_{f-s} = m_f\ddot{x} + c_f\dot{x} + k_f x \tag{6}$$

If the CFD/CSD simulation is perturbed such that x is held constant at $x=x_0$ while $\dot{x}$ and $\ddot{x}$ and are zero, then the remaining terms become:

$$k_f = -\frac{(F_{f-s})}{x_0} \tag{7}$$

With the known x_0, and F_{f-s} from the CFD/CSD simulation, k_f can be found from Equation (6). For the extraction of the fluid modal mass and damping, the system is instead driven at:

$$x = x_0 sin(\omega t) \tag{8}$$

which results in a response of the form:

$$-F_{f-s} = F_0 * sin(\ \omega t + \theta) \tag{9}$$

F_0 and the phase shift, θ, can be directly computed by comparing the input displacement and resulting force. The response can be represented as:

$$-(F_0\, sin(\omega t)\, cos(\theta) + F_0\, cos(\omega t)\, sin(\theta)) = (-m_f\omega^2 + k_f)x_0\, sin(\omega t) + c_f\omega x_0\, cos(\omega t) \tag{10}$$

Grouping similar terms result in equations for the modal mass and modal damping as follows.

$$m_f = -\frac{F_0\, cos(\theta) - x_0 k_f}{(-x_0\omega^2)} = -\frac{F_0\, cos(\theta) - x_0 k_f}{\ddot{x}} \tag{11}$$

$$c_f = -\frac{F_0\, sin(\theta)}{\dot{x}} \tag{12}$$

Multiple DOF Structural Modal Representation

First, the dynamic Equation for an elastic structure can be generally written as:

$$[M]\{\ddot{x}\}+[C]\{\dot{x}\}+[K]\{x\}=\{F\} \tag{13}$$

where [M] is a mass matrix, [C] is the damping matrix, [K] is the stiffness matrix, and {F} is a force vector. The above Equation can be transformed into modal space using:

$$\{x\}=[\Phi]\{Z\}=(\{\phi_1\},\{\phi_2\},...\{\phi_n\})\begin{Bmatrix} z_1 \\ z_2 \\ . \\ . \\ z_n \end{Bmatrix}=\sum_{i=1}^{n} Z_i\{\phi_i\} \tag{14}$$

where $[\Phi]$ is the modal matrix that contains modal shape vector $\{\varphi_i\}$, and Z_i is the modal displacement.

With the modal shape defined, we can substitute Eq. (14) into Eq. (13) to get:

$$[M_z]\{\ddot{Z}\}+[C_z]\{\dot{Z}\}+[K_z]\{Z\}=[\Phi]^T\{F\} \tag{15}$$

$[M_z]$, $[C_z]$, and $[K_z]$ are all diagonal matrices, representing the structural modal mass, modal damping, and modal stiffness. The right-hand side of Eq. (15) is the generalized force. As the left-hand side of the above Equation is decoupled, we can write each mode as follows:

$$M_{Zi,i}\ddot{Z}_i + C_{Zi,i}\dot{Z}_i + K_{Zi,i}Z = \xi_i \qquad \xi_i = \Phi_{i,j}F_j \tag{16}$$

The above Equation is strikingly similar to Equation (1). The exception is that the mass, damping, and stiffness are now the local modal values, and the force is the generalized modal force. Now the generalized force is expressed as:

$$\xi_i = \xi_i^{rig} + (\xi_i - \xi_i^{rig}) \tag{17}$$

with the first term representing the generalized force acting on the rigid structure and the second term representing the generalized force due to structural modal displacement. Because of the complexity of the multi-degree-of-freedom problem, all fluid modal mass, damping, and stiffness must be considered. We write Eq. (16) as:

$$\xi_i = \xi_i^{rig} + (\xi_i - \xi_i^{rig}) = \xi_i^{rig} - M_{Zfi,j}\ddot{Z}_j - C_{Zfi,j}\dot{Z}_j - K_{Zfi,j}Z_j \tag{18}$$

Or, in matrix form,

$$\{\xi\}=\{\xi^{rig}\}-[M_{Zf}]\{\ddot{Z}\}-[C_{Zf}]\{\dot{Z}\}-[K_{Zf}]\{Z\} \tag{19}$$

Now, our final equation becomes:

$$[M_Z + M_{Zf}]\{\ddot{Z}\}+[C_Z + C_{Zf}]\{\dot{Z}\}+[K_Z + K_{Zf}]\{Z\}=[\Phi]^T\{F^{rig}\} \tag{20}$$

Extraction of Fluid Modal Stiffness, Mass, and Damping for Multiple DOF

To extract the fluid properties in modal space, a similar procedure can be applied. The steps are as follows:

1. Select the first M modes from a structural solver (for example, NASTRAN or CoBi). Output the modal shape vectors $\{\Phi_i\}$.
2. Define a modal displacement: $Z_i = Z_{io}$
3. Impose boundary conditions on the boundary of the CFD grid through modal shape for the i^{th} mode: $\{x_i\} = Z_{io}(\Phi_i)$
4. Solve a fluid dynamics problem using a CFD solver with the above boundary condition. Find the modal force for all M modes: $\xi_j = \{\Phi j\}^T \{F\}$, j=1,... M
5. Determine the fluid modal stiffness:

$$K_{zfi,j} = -\frac{\xi_j}{Z_{i0}} \tag{21}$$

6. Define a modal displacement: $Z_i = Z_{i0}\sin(\omega_i t)$
7. Impose boundary condition on the boundary of the CFD grid through modal shape for the i^{th} mode: $\{x_i\} = Z_{i0}(\Phi_i)\sin(\omega_i t)$, with ω_i as the i^{th} modal frequency.
8. Solve a fluid dynamics problem using a CFD solver with the above boundary condition. Find the modal force for all M modes: $\xi_j = \{\Phi j\}^T \{F\}$, j=1,... M
9. Determine the fluid modal mass and damping:

$$M_{zfi,j} = -\frac{\zeta_j\, cos(\theta) - K_{zfi,j} Z_{i0}}{-\omega^2 Z_{io}},\ \ C_{Zfi,j} = -\frac{\zeta_j\, sin(\theta)}{\omega Z_{i0}} \tag{22}$$

Formulations of Full-Coupled Fluid-Structure Interaction Problem into an ODE Equation.

The simulation was conducted for AGARD 445.6 wing for freestream dynamic pressures of q=50 and q200. The resulting matrices are shown in Table 1 for q=50 and q=200.

Table 1. Extracted fluid modal properties for AGARD 445.6 wing at freestream dynamic pressure q, (a) q=50, (b) q=200.

(a) q=50

Mass x 10^{-4}	Mode 1	Mode 2	Mode 3	Mode 4
Mode 1	7.6618	-16.4514	9.5289	-2.2855
Mode 2	2.9870	-12.6031	9.0445	-1.4567
Mode 3	0.64317	2.5442	7.2457	-0.5248
Mode 4	1.0599	-9.1680	1.8544	8.4162

Damping	Mode 1	Mode 2	Mode 3	Mode 4
Mode 1	0.7468	-1.6001	0.7399	0.5895
Mode 2	0.3678	1.7523	-0.2280	-1.4237
Mode 3	0.1170	-1.0279	1.2949	-1.3615
Mode 4	-0.0402	0.6915	-0.1282	1.3034

Stiffness	Mode 1	Mode 2	Mode 3	Mode 4
Mode 1	145.55	-1171.58	543.05	827.49
Mode 2	158.13	-883.59	689.12	-1205.96
Mode 3	13.38	-203.67	314.50	-302.32
Mode 4	39.42	-93.01	223.54	-348.99

(b) q=200

Mass x 10^{-4}	Mode 1	Mode 2	Mode 3	Mode 4
Mode 1	29.9568	-64.9992	38.0797	-9.1326
Mode 2	11.0928	-49.4313	36.0569	-5.8124
Mode 3	2.4765	10.1724	28.9927	-2.0804
Mode 4	3.8380	-36.3381	7.3866	33.6465

Damping	Mode 1	Mode 2	Mode 3	Mode 4
Mode 1	3.0077	-6.4109	2.9604	2.3574
Mode 2	1.4703	7.0036	-0.9097	-5.6928
Mode 3	0.4745	-4.1025	5.1809	-5.4449
Mode 4	-0.1605	2.7559	-0.5129	5.2192

Stiffness	Mode 1	Mode 2	Mode 3	Mode 4
Mode 1	582.64	-4686.32	2172.22	3309.99
Mode 2	632.52	-3534.35	2756.47	-4823.83
Mode 3	53.50	-814.69	1258.02	-1209.28
Mode 4	157.70	-372.08	894.15	-1395.96

One notices that all the components of the matrix are proportional to q. We only need to extract the matrix for one value of q and obtain the rest using the above feature. With the extracted fluid mass, damping, and stiffness, the modified structural Equation (20) can be written as:

$$\left\{\underbrace{\begin{bmatrix}1&&&\\&1&&\\&&1&\\&&&1\end{bmatrix}}_{\text{Existing in structural modal solver}}+\underbrace{\begin{bmatrix}m_{11}&m_{12}&m_{13}&m_{14}\\m_{21}&m_{22}&m_{23}&m_{24}\\m_{31}&m_{32}&m_{33}&m_{34}\\m_{41}&m_{42}&m_{43}&m_{44}\end{bmatrix}}_{\text{Extracted from CFD}}\right\}\begin{Bmatrix}\ddot{Z}_1\\\ddot{Z}_2\\\ddot{Z}_3\\\ddot{Z}_4\end{Bmatrix}+\left\{\underbrace{\begin{bmatrix}c_{11}&c_{12}&c_{13}&c_{14}\\c_{21}&c_{22}&c_{23}&c_{24}\\c_{31}&c_{32}&c_{33}&c_{34}\\c_{41}&c_{42}&c_{43}&c_{44}\end{bmatrix}}_{\text{Extracted from CFD}}\right\}\begin{Bmatrix}\dot{Z}_1\\\dot{Z}_2\\\dot{Z}_3\\\dot{Z}_4\end{Bmatrix}+\left\{\underbrace{\begin{bmatrix}\omega_1^2&&&\\&\omega_2^2&&\\&&\omega_3^2&\\&&&\omega_4^2\end{bmatrix}}_{\text{Existing in structural modal solver}}+\underbrace{\begin{bmatrix}k_{11}&k_{12}&k_{13}&k_{14}\\k_{21}&k_{22}&k_{23}&k_{24}\\k_{31}&k_{32}&k_{33}&k_{34}\\k_{41}&k_{42}&k_{43}&k_{44}\end{bmatrix}}_{\text{Extracted from CFD}}\right\}\begin{Bmatrix}Z_1\\Z_2\\Z_3\\Z_4\end{Bmatrix}=[\Phi]^T\left\{F^{rig}\right\} \tag{23}$$

Now the coupled fluid-structure problem has been decoupled into an ODE problem.

2.3 Reduction of Flutter Boundary Determination into an Algebraic Problem

From the above analysis, we can make the following simplifications:

1. The fluid modal mass contributions can be neglected as they are 4 orders of magnitude smaller than the structural mass.
2. Fluid damping can be neglected, as it is less than 1%.
3. The fluid modal stiffness for mode 3 and mode 4 can be neglected as they are much smaller than the structural stiffness. So, mode 3 and mode 4 can be decoupled from the aeroelastic equation.
4. Define: $k_{11}=\kappa_{11}q$; $k_{12}=\kappa_{12}q$; $k_{21}=\kappa_{21}q$; $k_{22}=\kappa_{22}q$

Now, equation (23) can be reduced further to the eigenvalues of 2 ODE of:

$$\begin{bmatrix} 1 & 0 \\ 0 & 1 \end{bmatrix} \begin{Bmatrix} \ddot{x}_1 \\ \ddot{x}_2 \end{Bmatrix} + \begin{bmatrix} {\omega_1}^2 + \kappa_{11} q & \kappa_{12} q \\ \kappa_{21} q & {\omega_2}^2 + \kappa_{22} q \end{bmatrix} \begin{Bmatrix} x_1 \\ x_2 \end{Bmatrix} = 0 \tag{24}$$

All the off-diagonal terms are due to fluid modal contribution. By setting:

$$x_j = x_{j_0} e^{irt}; \qquad \ddot{x}_j = -r^2 x_{j_0} e^{irt};\ j = 1,2 \tag{25}$$

The determinant of the above 2x2 eigenvalue problem becomes:

$$\left(-r^2 + {\omega_1}^2 + \kappa_{11} q\right)\left(-r^2 + {\omega_2}^2 + \kappa_{22} q\right) - \kappa_{12} \kappa_{21} q^2 = 0 \tag{26}$$

The solution gives:

$$r^2 = \frac{1}{2}\left[\left({\omega_2}^2 + \kappa_{22} q + {\omega_1}^2 + \kappa_{11} q\right) \pm \sqrt{\left({\omega_2}^2 + \kappa_{22} q - {\omega_1}^2 - \kappa_{11} q\right)^2 + 4 k_{12} k_{21} q^2}\right] \tag{27}$$

One can see that since $\kappa_{12} < 0$ and $\kappa_{21} > 0$, there is a critical q value that leads to:

$$\left({\omega_2}^2 + \kappa_{22} q - {\omega_1}^2 - \kappa_{11} q\right)^2 + 4 k_{12} k_{21} q^2 = 0 \tag{28}$$

The critical flutter frequency is then:

$$r = \sqrt{\frac{1}{2}\left({\omega_1}^2 + {\omega_2}^2 + \kappa_{11} q + \kappa_{22} q\right)} \tag{29}$$

First, we notice that if $\kappa_{12}\kappa_{21} \equiv 0$, the two roots from equation (28) are:

$$r_1 = \pm\sqrt{{\omega_1}^2 + \kappa_{11} q}; \qquad r_2 = \pm\sqrt{{\omega_2}^2 + \kappa_{22} q} \tag{30}$$

For M=0.5, the κ values are listed in Table 2 below:

Table 2. Fluid Stiffness Value for the First Two Structural Modes

κ	κ_{11}	κ_{12}	κ_{21}	κ_{22}
Extracted Value	2.911	-23.43	3.16	-17.66

We can see that k22 is negative, which has the potential to lead to flutter. But in our problem $\kappa_{12}\kappa_{21} < 0$, this term is more important, as seen from equation (27). The mechanism leading to flutter $\kappa_{12}\kappa_{21} < 0$ is illustrated in Figure 5. With a small perturbation in mode 1 δx_1, a force on mode 2 is induced, which is $\kappa_{12} q * \delta x_1$. This force will generate a mode displacement x_2. Again, the mode 2 displacement will generate a force on mode 1 $\kappa_{21} q * \delta x_2$, which will lead to mode 1 displacement. When $\kappa_{12}\kappa_{21} < 0$, there is potential to lead to the continuous growth of the mode displacement, and hence the flutter.

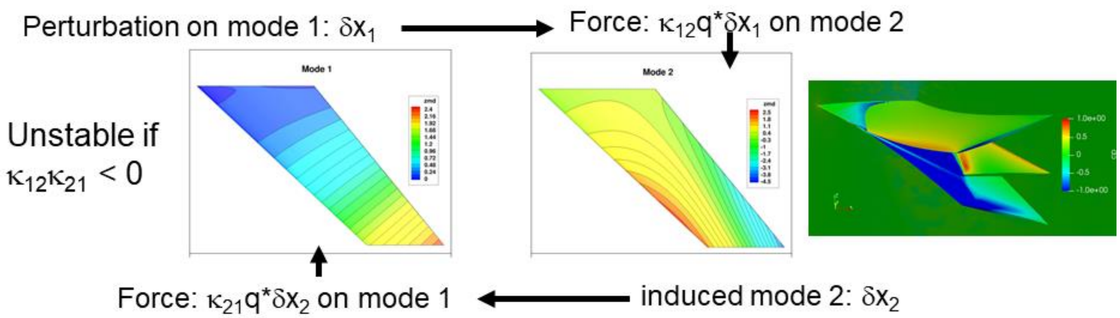

Figure 5. The mechanism leading to flutter due to fluid stiffness

As for the accuracy of the algebraic expression (28), the comparison with experimental data is shown in Figure 6. One can see that:

- For subsonic flow, the algebraic equation gives a good agreement with fully coupled FSI and experimental data. For transonic and supersonic flow, the algebraic equation over-predicts flutter boundary.
- As derived, the flutter frequency falls between the first and second structural modal frequencies (Figure 7).
- The algebraic equation model can provide a quick estimate of flutter boundary, and it only needs two steady-state extractions: one for k11 and k21 and one for k21 and k22.

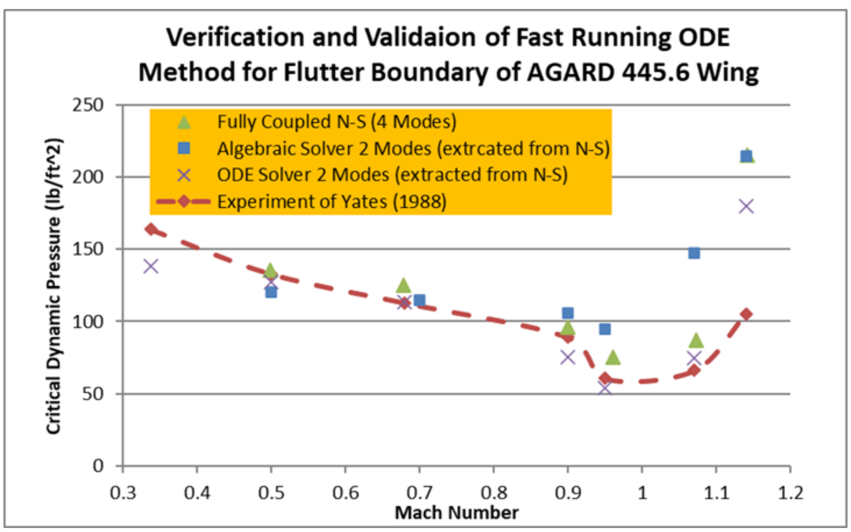

Figure 6. Validation of fast running fluid modal method extracted from N-S solver for the prediction of flutter dynamic pressure boundary of an AGARD 445.6 wing using the developed algebraic solver with two modes.

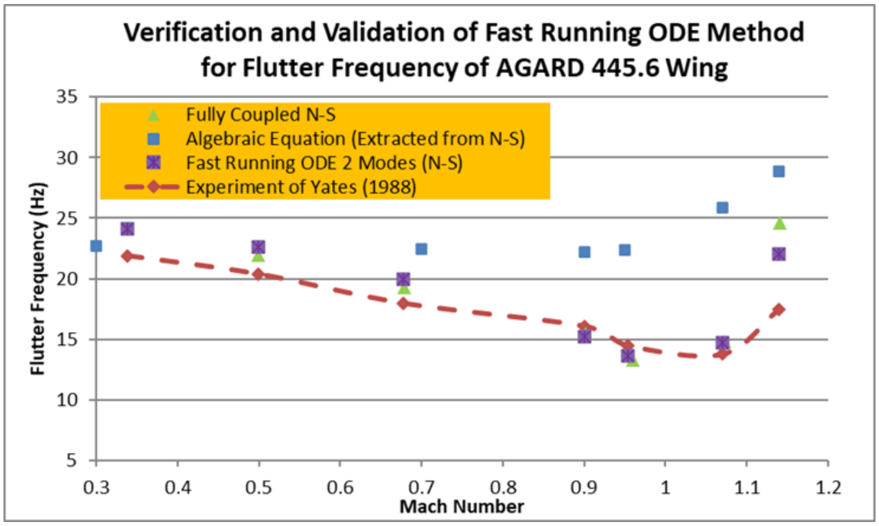

Figure 7. Validation of fast running fluid modal method extracted from N-S solver for the prediction of flutter frequency boundary of an AGARD 445.6 wing using the algebraic expression from the first two structural modes.

2.4 Efficient Flutter Prediction of F-16 Mode Using Fluid Modal Method

In the following, we will demonstrate our procedure for obtaining the flutter boundary for the F-16 model.

Extraction of Stiffness Matrix

First, the fluid stiffness is extracted by displacing each mode by a specified value x_0 and holding that modal displacement until a steady-state solution is reached. An appropriate value for x_0 can be approximated using the following equation:

$$\frac{mode\ 1\ maximum\ displacement\ at\ wing\ tip}{wing\ span} * x_0 = 1\% \tag{31}$$

This ramp and hold simulation was conducted for each mode individually at the specified freestream conditions. A "zero perturbation" simulation was also executed to obtain the modal load biases. This was achieved by forcing all the modes in the system to stay at an amplitude of 0 until a steady-state solution was reached. All simulations were conducted using the SA (Spalart-Allmaras) turbulence model.

Once the modal force is obtained, the stiffness is calculated using the following equation:

$$k_f = \frac{-(F_{f-s} - F_{bias})}{x_0}$$

F_{f-s} is the resulting modal load for each mode. F_{bias} is the resulting modal load of each mode from the "zero perturbation" simulation. Upon reaching a steady-state these modal loads values are extracted, and the nonlinear fluid modal stiffness is calculated. Table 3 shows the format of the modal stiffness matrix.

Table 3. Format of the Fluid Modal Stiffness Matrix

k_f	Mode 1	Mode 2	…
Mode 1	Mode 1 response to Mode 1 displacement	Mode 1 response to Mode 2 displacement	…
Mode 2	Mode 2 response to Mode 1 displacement	Mode 2 response to Mode 2 displacement	…
…	…	…	…

Table 4 presents the resulting fluid modal stiffness matrix of the Open Source Fighter.

Table 4. Fluid Modal Stiffness Matrix of Open Source Fighter at M = 0.96 and Q = 27kPA

k_f	Mode 1	Mode 2	Mode 3	Mode 4	Mode 5	Mode 6	Mode 7	Mode 8	Mode 9	Mode10
Mode1	-21.25	-3.75	-3.75	26.25	-2.5	-3.75	162.5	1.25	162.5	-1.25
Mode2	0	76.25	-65.75	0	0	-3	0	-215	0	173.75
Mode3	0	57.5	-31.625	0	0	-1.875	0	-129.5	0	72.25
Mode4	-27.5	0	0	-262.5	0	0	-87.5	0	-3.75	0
Mode5	-0.625	-0.2	-0.125	-0.4625	-0.125	-0.125	2.5	-0.0625	3	-0.125
Mode6	0	-1.0875	0	0	0	-0.3375	0	2.8375	0	-1.1625
Mode7	-56.25	-1.25	-0.5	-105	0	0	178.75	8.75	278.75	1.25
Mode8	0	-105	100	0	5.625	5.625	0	290	0	-257.5
Mode9	-48.75	0	0	-156.25	0	0	12.5	0	145	0
Mode10	0	-34.625	-7.7	0	0.875	0.875	0	53.375	0	-6.6

Identification of Mode Coupling

The possible coupling modes are identified by the color marks. These modes are coupled because they have opposite signs in the off-diagonal terms. These are highlighted in the table above and listed here:

- $k_{1,4}$ and $k_{4,1}$
- $k_{1,7}$ and $k_{7,1}$
- $k_{1,9}$ and $k_{9,1}$
- $k_{2,3}$ and $k_{3,2}$
- $k_{2,10}$ and $k_{10,2}$
- $k_{3,8}$ and $k_{8,3}$
- $k_{3,10}$ and $k_{10,3}$
- $k_{5,8}$ and $k_{8,5}$
- $k_{5,10}$ and $k_{10,5}$
- $k_{6,10}$ and $k_{10,6}$
- $k_{8,10}$ and k_{10}

Calculate the Critical Q Values and Frequencies

Our fluid modal method needs the following inputs for each modal coupling: omega1, omega2, kappa11, kappa12, kappa21, kappa22, and g_{mass}. Where 1 represents the first mode of the coupling and 2 the second. The equations for these inputs are as follows:

- $\omega_x = 2 * \pi * f_{x1}$, where f_{x1} is the natural frequency of mode x,
- $\kappa_{xx} = k_{xx}/Q$, where k_{xx} comes from the stiffness matrix and Q is the dynamic pressure,
- and g_{mass} is the generalized mass term and for this case it has a value of 1.

The algebraic equation for the Nonlinear Fluid Model Method is as follows:

$$r^2 = \underbrace{\frac{1}{2}[(\omega_2{}^2 + \kappa_{22} q + \omega_1{}^2 + \kappa_{11} q)}_{\text{Flutter Frequency}} \pm \underbrace{\sqrt{\left(\omega_2{}^2 + \kappa_{22} q - \omega_1{}^2 - \kappa_{11} q\right)^2 + 4k_{12} k_{21} q^2}]}_{\text{Flutter Q Value}}$$

Solving for r (root) will result in a pair of critical Q values (due to the ±) which can then be used to calculate corresponding critical frequencies. If a Q value is negative, it is expected not to exist, but this will need verification.

The output of the Nonlinear Fluid Modal Method for the Open Source Fighter is shown in Table 5. Note that the – and + represent the solution by using either the – or + before the square root in the equation. All cells highlighted in grey either have a negative Q value or a corresponding frequency that resulted in *NAN* (not a number). The modal couplings with these results are expected to not occur.

Table 5. Results of the Nonlinear Fluid Modal Method

Coupled Modes	$\boldsymbol{Q-}$	$\boldsymbol{Q+}$	$\boldsymbol{f-}$	$\boldsymbol{f+}$
$k_{1,4}$ and $k_{4,1}$	75,919	119,431	3.8	2.9
~~**$k_{1,7}$ and $k_{7,1}$**~~	-12,989,777	-291,754	*NAN*	6.8
$k_{1,9}$ and $k_{9,1}$	10,737,977	-366,807	26.4	7.2
$k_{2,3}$ and $k_{3,2}$	24,107	-368,578	4.8	3.9
$k_{2,10}$ and $k_{10,2}$	783,993	-2,581,353	11.5	4.8
~~**$k_{3,8}$ and $k_{8,3}$**~~	-1,186,052	-203,057	*NAN*	7.3
~~**$k_{3,10}$ and $k_{10,3}$**~~	8,172,596	-2,507,093	*NAN*	12.5
~~**$k_{5,8}$ and $k_{8,5}$**~~	-243,563	-241,580	8.0	8.0
$k_{5,10}$ and $k_{10,5}$	19,597,892	24,057,391	8.2	7.3
$k_{6,10}$ and $k_{10,6}$	16,621,896	32,417,051	8.7	5.0
$k_{8,10}$ and $k_{10,8}$	130,838	1,118,370	13.4	17.6

Based on our theory, the possible mode couplings sorted in ascending Q value (dynamic pressure) are shown in Table 6. From the table, it can be seen that at a dynamic pressure of 24K, one can expect modes 2 and 3 to be coupled together and have a coupling frequency of 4.8 Hz. Even though several other mode couplings are listed, this coupling is the most important since it will occur first.

Table 6. Possible Mode Couplings of the Open Source Fighter

Coupled Modes	Q	f
$k_{2,3}$ and $k_{2,3}$	24 kPa	4.8 Hz
$k_{1,4}$ and $k_{4,1}$	76 kPa	3.8 Hz
$k_{1,4}$ and $k_{4,1}$	119 kPa	3.0 Hz
$k_{8,10}$ and $k_{10,8}$	131 kPa	13.4 Hz
$k_{2,10}$ and $k_{10,2}$	784 kPa	11.5 Hz
$k_{8,10}$ and $k_{10,8}$	1.1 MPa	17.6 Hz
$k_{1,9}$ and $k_{9,1}$	10.7 MPa	26.4 Hz
$k_{6,10}$ and $k_{10,6}$	16.6 MPa	8.7 Hz
$k_{5,10}$ and $k_{10,5}$	19.6 MPa	8.2 Hz
$k_{5,10}$ and $k_{10,5}$	24 MPa	7.3 Hz
$k_{6,10}$ and $k_{10,6}$	32.4 MPa	5.0 Hz

2.5 Verification of Predicted Flutter Values Using Fully Coupled Solution

The fully coupled FSI simulation will be used to verify the accuracy of the nonlinear fluid modal method. The fully coupled aeroelastic simulation can be conducted in two steps: 1) obtaining a steady-state solution of the flow field and 2) ping the structure (start of FSI) and observing the unsteady response.

Steady-State Solution

Obtaining a steady-state solution ensures a good initial condition before any structural motion occurs. This can be done by running a fully coupled CFD and structural code with global time-stepping or by using a larger time-step with startup iterations with local time stepping. An example steady-state solution result can be seen in Figure 8. The free-stream conditions of this case are: Mach = 0.96, Q = 60 kPa, Density = 0.6 kg/m^3, Velocity = 447 m/s, and Altitude = 717 m. Note that the dynamic pressure for this example is a little more than double that which was used for extracting the stiffness matrix. Lift, drag, and pitch coefficients are all converged. As expected, several shocks are present in the flow field along the fuselage and on the wing.

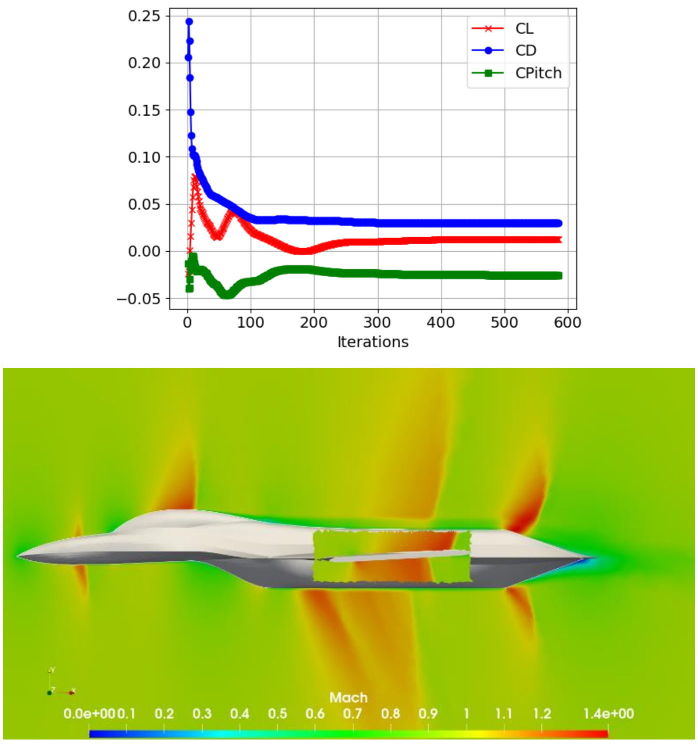

Figure 8. Steady-State Flow Field and Convergence Properties of the Q = 60 kPa Run

Ping the Structure and Observe the Unsteady Response
The structure can be "pinged" by supplying an initial velocity to all modes. With the ping, each mode will begin to oscillate. After some time, the modes will either decay or grow. The modes that grow are unstable. For example, the modal displacements of Modes 2 and 3 for the same case from Figure 8 are shown in Figure 9. The predicted critical Q value for flutter onset was calculated to be 24 kPa. Since the simulation was conducted well above that region at a dynamic pressure of 60 kPa, one should expect the modes that lead to instability to grow without bound, as shown in Figure 9.

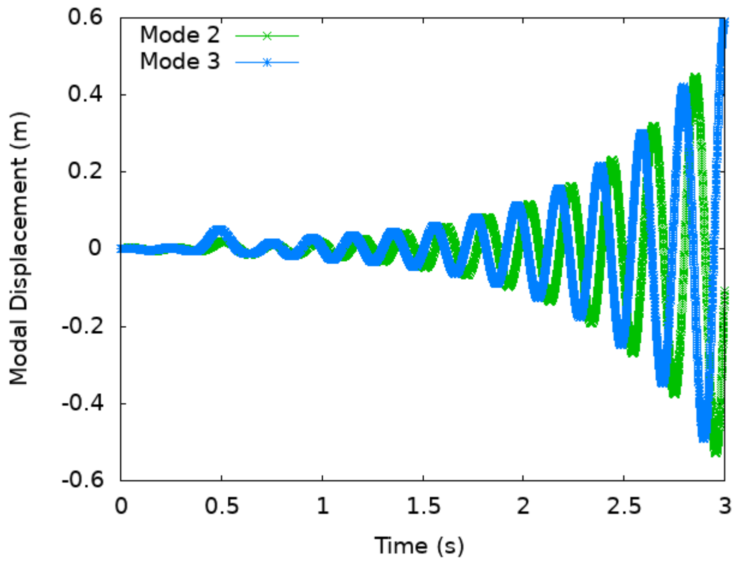

Figure 9. Modal Displacements of Modes 2 and 3 for the Q = 60 kPa Run

2.6 *Capturing the Critical Q value and Frequency of Flutter Onset*

For this study, flutter was defined as when the coefficient of Roll of the simulation resulted in a damping factor of zero. A total of 8 dynamic pressure values ranging from 10 kPa to 60 kPa were simulated to narrow in on the critical Q value. Figure 10 shows the damping factors of the 27.5 kPa, 30 kPa, and 35 kPa runs. A quadratic fit was employed to extrapolate the critical Q value. The critical Q value extrapolated from the simulation runs is very close to that predicted by the nonlinear fluid modal method, resulting in a percent error of less than 2%. To determine the flutter frequency, the FFT (fast Fourier transform) of the coefficient of Roll of the Q = 40 kPa simulation run is shown in Figure 11. The theoretical critical frequency determined by the nonlinear fluid modal method was 4.8 Hz, as given in Table 7. The plot of Figure 11, which determines the frequency content of the cRoll data, shows a peak at 4.8 Hz as well.

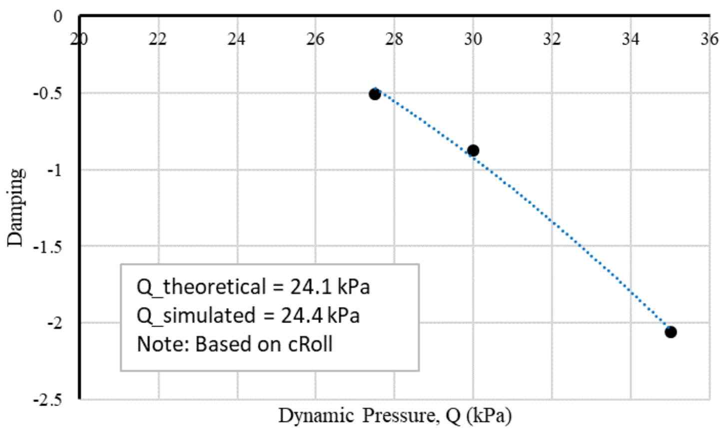

Figure 10. Extrapolation of the Simulated Critical Q Value of the Open Source Fighter at Mach = 0.96

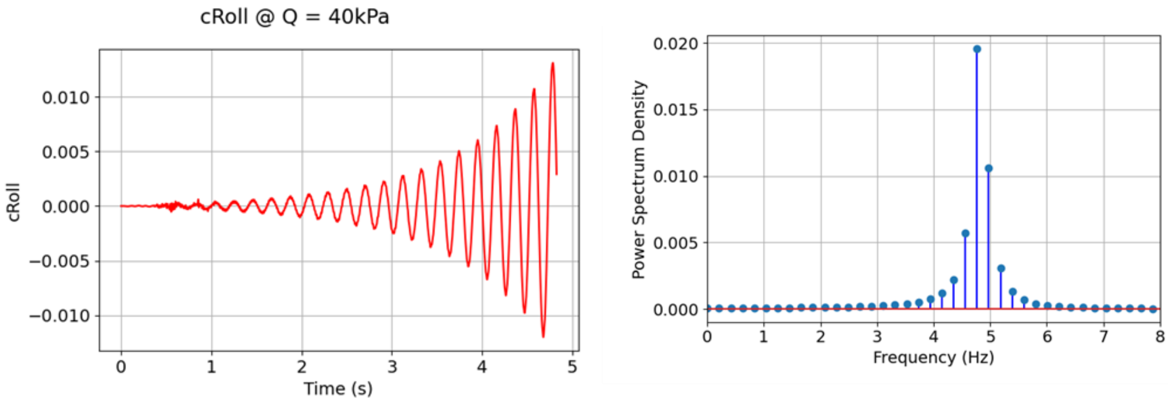

Figure 11. FFT of the Coefficient of Roll of the Q = 40 kPa Simulation Run

Table 7 shows the comparison of dynamic flutter pressure and flutter frequency from the fully coupled solution and the current fluid modal method. One can see very good agreements.

Table 7. Comparison of Flutter Dynamic Pressure and Flutter Frequency

	Current Fluid Modal Method	Fully Coupled Solution
Flutter Dynamic Pressure (kPa)	24.1	24.4
Flutter Frequency (Hz)	4.80	4.80

2.7 <u>Prediction of Flutter Boundary</u>

All results up to this point have only been dealing with the onset of flutter at a Mach number of 0.96. However, from past aeroelastic analysis, the critical Q value has been shown to be dependent on the Mach number. Several methods for predicting flutter have been developed over the years. One such method, known as the Schur method, was implemented in the Open-Source Fighter Geometry by Marques *et al.* [6]. These results are presented in Figure 12, along with the calculated critical Q value determined by the nonlinear fluid modal method. Since the Schur method included Euler solutions, the stiffness matrices for each Mach number were extracted using an Euler solver. As seen in the figure, the nonlinear fluid modal method compares well with the Shur method. The critical Q values calculated for the nonlinear fluid modal method were determined using only the coupling between Mode 2 and Mode 3.

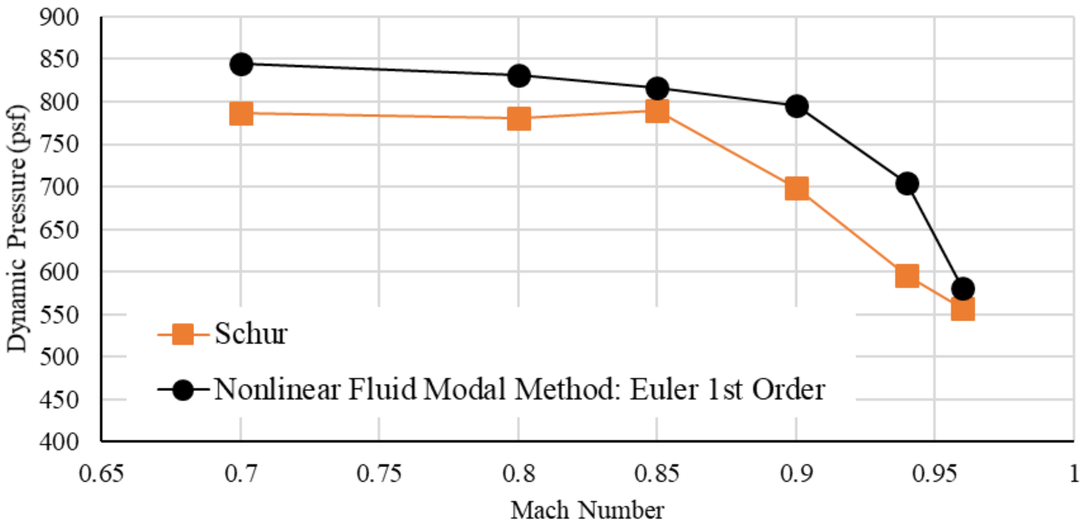

Figure 12. Flutter Boundary for the Open-Source Fighter with Comparisons between the Schur and Nonlinear Fluid Modal Methods

3 Conclusion and Future Work

An innovative "nonlinear fluid modal method" is presented to rapidly predict and offer unique physical insight into the nonlinear aeroelasticity of aircraft. The distinguishing factors of this effort are: (1) It is physics-based so that changes in aerodynamics, mass, inertia, and center of gravity are accounted for. (2) It is time-accurate and fast running. The coupled CFD/CSD problem is reduced to a set of ordinary differential equations, which can be solved in a matter of seconds compared to several hundred CPU hours. (3) It is CFD/CSD code independent. Any existing CFD solver can be used to build the nonlinear fluid modal model. (4) It is applicable to any geometry and flight condition.

References

[1] Silva, W.A. and Bartels, R.E. "Development of Reduced-Order Models for Aeroelastic Analysis and Flutter Prediction Using the CFL3Dv6.0 Code," J. Fluids Struct. 2004, 19, 729-745.

[2] Silva, W.A., Vasta V.N., and Biedron, R.T. "Development of Unsteady Aerodynamic and Aeroelastic Reduced-Order Models Using the FUN3D Code," 2009, IFASD Paper No. 2009-30.

[3] H. Q. Yang, Timothy Wray, Simon Yang, and Henry Ran, "The Nonlinear Fluid Modal Method for Efficient Dynamic Aeroelastic Simulation," AIAA SciTech, January 3-7, 2022, San Diego. AIAA 2022-2503.

[4] Hongjun Ran, Tim Wray, Simon Yang and Hong Q. Yang "Time Marching Aeroelasticity Modeling and Validation Study for Plates with and without Hole," AIAA SciTech, January 6-10, 2020. AIAA 2020-2289

[5] Jason C. Howison and H.Q. Yang, "Fully-Coupled LCO Predictions for a Flat Plate in Low-Speed Flow," AIAA SciTech, January 3-7, 2022, San Diego. AIAA 2022-0653.

[6] Marques S, Badcock KJ, Khodaparast HH, Mottershead JE. Transonic aeroelastic stability predictions under the influence of structural variability. Journal of Aircraft 2010;47(4):1229–39.